Bayesian Gaussian Processes for Coordinate-based Meta-analysis of Neuroimaging Reports

Reza Salimi-Khorshidi[1], Stephen M. Smith[1], Thomas E. Nichols[2,1], Mark W. Woolrich[3,1]

[1] Oxford University Centre for Functional MRI of the Brain (FMRIB), Oxford, UK
[2] University of Warwick, Coventry, UK
[3] Oxford University Centre for Human Brain Activation (OHBA), Oxford, UK

Introduction

Current coordinate-based meta-analyses (CBMA) of neuroimaging studies utilize relatively sparse information from published studies, typically only using (x,y,z) coordinates of the activation peaks. Such CBMA methods have several limitations [1].
First, there is no way to jointly incorporate deactivation information when available, which has been shown to result in an inaccurate statistic image when assessing a difference contrast [2]. **Second**, the scale of a kernel reflecting spatial uncertainty must be set either arbitrarily or without taking the effect size (e.g., Z-stat) into account. To address these problems, we employ Gaussian-process regression (GPR), *explicitly* estimating the unobserved statistic image given the sparse peak activation "coordinate" and "standardized effect-size estimate" data. In particular, our model allows meta-level estimation of standardized effect size at each voxel, something existing CBMA methods cannot produce.
Our results show that GPR outperforms existing CBMA techniques (such as ALE and KDA) and is capable of more accurately reproducing the (usually unavailable) full-image analysis results.

Methods

Suppose the full-image study-level data were available, then for study s at voxel k, the contrast estimates can be modelled as Equation 1. Typically CBMA does not have access to y and t at every voxel; instead it has access to sparsely-sampled z=y/t image, which changes the model to Equation 2. If we assume that for every study, image t is almost identical (i.e., studies are similarly reliable in their effect-size estimates), then the model is as Equation 3.
Even though CBMA only has access to n sparsely-located samples of Z-image ($\boldsymbol{z}$=$(z_1,z_2,...,z_n)$) with their corresponding voxel coordinates $\boldsymbol{V} = \{\mathbf{v}_1, \mathbf{v}_2, \ldots, \mathbf{v}_n\}$, we can employ GPR to model those voxels' (unobserved) standardized mean effect size m. Under GPR, m is assumed to be a sample from a Gaussian process described as $m \sim \mathrm{N}(0,\boldsymbol{C})$, with $\boldsymbol{C}$ denoting the covariance matrix of the process. We employ a squared exponential (SE) covariance function whose shape depends on two hyperparameters σ_f (describing m's variance) and λ (describing m's smoothness). Assuming that z is sampled from m with Gaussian noise $\mathrm{N}(0,\sigma_n^2)$ results in Equation 4 (see Figure 1 for an illustrative example).
In the first step of this solution (inference), the model's hyperparameters (σ_n, σ_f, and λ) are estimated with evidence optimization (EO), and used in the second step (prediction) to result in m at n^* new voxels [1]. We incorporate our prior knowledge about statistic images' smoothness by employing a Gamma prior (with mean 1 and SD of 5 voxels) on λ and fixing σ_f at 3 voxels [1],

Equation 1 :

$$y_{s,k} = \mu_k + w_{s,k}, \text{ where } w_{s,k} \sim \mathcal{N}(0, t_{s,k}^2 + g_k^2)$$

μ_k : the overall population mean effect at voxel k

$w_{s,k}$: the error at study s and voxel k

$t_{s,k}$: within − study variance

g_k : inter − study variance

Equation 2 :

$$z_{s,k} = \frac{\mu_k}{t_{s,k}} + e_{s,k}, \text{ where } e_{s,k} \sim \mathcal{N}(0, 1 + g_k^2/t_{s,k}^2)$$

Equation 3 :

$$z_{s,k} = m_k + e_{s,k}, \text{ where}$$
$$e_{s,k} \sim \mathcal{N}(0, 1 + v_k^2),\ m_k = \mu_k/t_k \text{ and } v_k^2 = g_k^2/t_k^2$$

Equation 4 :

$$z_k \sim \mathcal{N}(m_k, \sigma_n^2)$$

where σ_n estimates $1 + g_k^2/t_{s,k}^2$, and $m \sim \mathcal{GP}(0, C)$

Figure 1: GP Toy Illustration. The left panel shows three functions drawn at random from a GP prior; while the the GP concerns functions, in practice we sample on a finite grid (indicated by the dots for one of the functions). The right panel shows three random functions drawn from the posterior, i.e., the process conditioned on the five noise-free observations indicated (y, with $\sigma_n = 0$, i.e., $y = f(x)$). In both plots the shaded area represents the point-wise mean plus and minus two times the standard deviation for each input value (corresponding to the 95% confidence region), for the prior (left) and posterior (right). In order to apply this concept to CBMA, we take the input $\boldsymbol{x}$ to be 3D coordinate values reported and the underlying effect-size image $f(\boldsymbol{x})$ prior can be sampled as a $\mathrm{GP}(0,\boldsymbol{C})$.

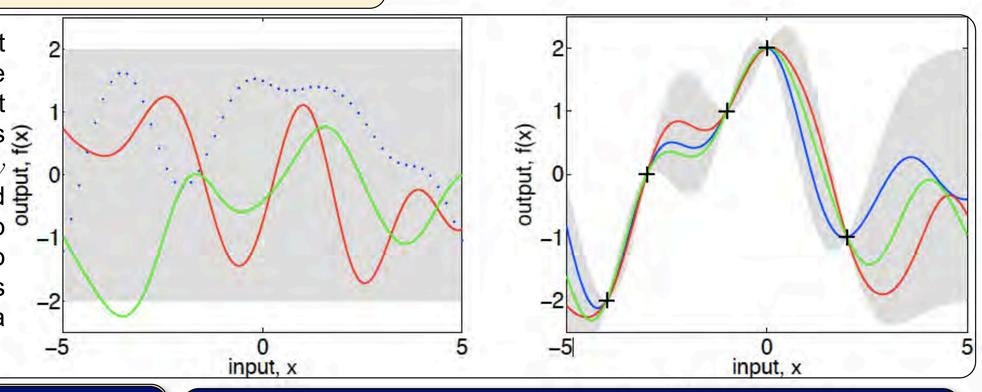

Results

We present evaluations of our GPR CBMA's performance when applied to both simulated and real data, as well as comparisons with image-based meta-analysis (IBMA) and CBMA (ALE and KDA) alternatives [1]. For IBMA, we employed mixed effect (MFX) and fixed effects (FFX) FLAME (FMRIB's local analysis of mixed effects), FSL's Bayesian tool for multi-level modeling of effect sizes.
Figure 2 illustrates the gold-standard Z-stat map together with the ones resulting from IBMA and CBMA. This Figure shows that the GPR handles data with both activation and deactivation more accurately than the other two methods.
Figure 3 quantifies the accuracy of the GPR, ALE and KDA under simulation when truth is known. While ALE and KDA can be tuned to optimize performance, here they never exceed the accuracy of the self-tuning GPR.
Figure 4 shows a meta-analysis of real data, consisting of a group of 20 fMRI study of pain (ALE σ=15mm; see [1] for full details) In IBMA, these studies are pooled under a mean/average contrast using both FLAME-FFX and FLAME-MFX. Like the simulated results, GPR appears more similar to IBMA results, and has little problem with bleeding activation results into deactivation results (when modelled separately).

Conclusions

In spite of minimal access to study-level image data, GPR is able to mimic IBMA results better than ALE or KDA. The improvements over existing methods are the ability to estimate the smoothing parameter from the data itself, as well as being able to simultaneously model activation and deactivation data.
The only significant limitation is that the Z-statistic peak values are needed in addition to the (x,y,z) coordinate data. While Z-stats are usually reported, they are sometimes missing; in those instances we imputation conservative values could be used to allow GRP to accommodate such studies as well.

Figure 3: Using the Dice Coefficient (DC) for evaluating the performance of CBMA methods when applied to the simulated 3D data. The left panel compares ALE and KDA against our advocated method (i.e., GPR using joint foci and prior on λ) and GPR with activation foci overlaid on GPR with deactivation foci mean (top panel) and difference (bottom panel) contrasts. The result indicates the GPR using joint foci performs better than ALE and KDA over a fairly-extensive range of their kernel sizes.

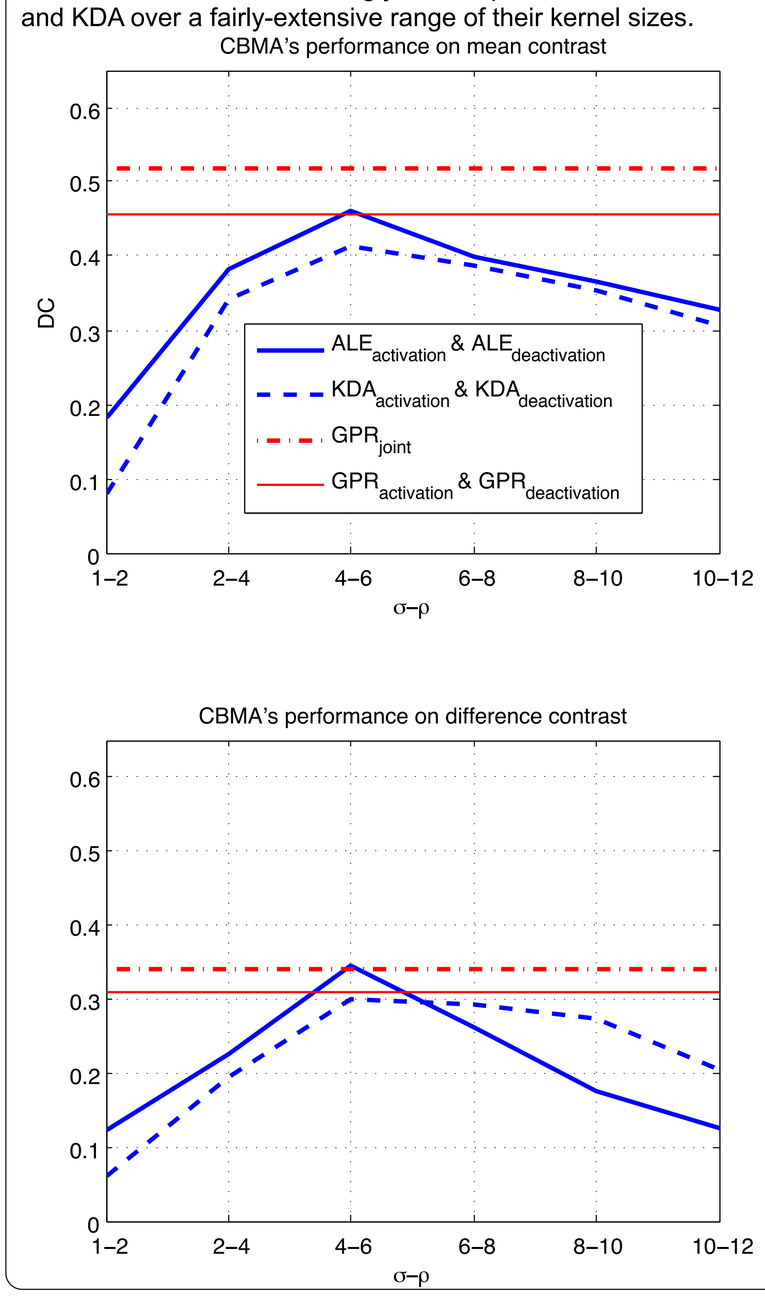

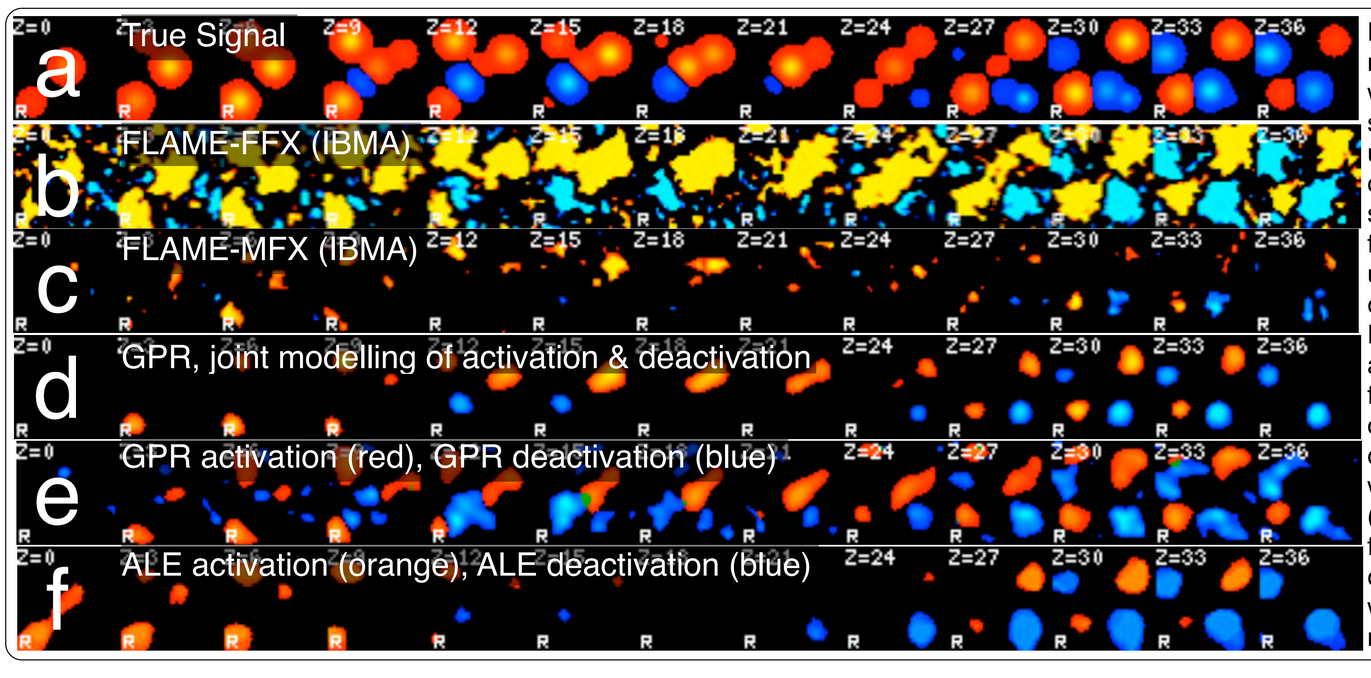

Figure 2: IBMA and CBMA results (i.e., Z-stat images) when pooling a set of 3D simulated studies. The underlying signal for the one-group simulation is shown in (a) with the results from pooling these studies under a mean/average contrast using FLAME-FFX, FLAME-MFX, GPR with joint activation and deactivation foci, GPR with activation foci overlaid on GPR with deactivation foci, and ALE with $\sigma = 4$ voxels, shown in (b)-(f), respectively. In this figure, red-yellow and blue colours show Z-stat values with range [2, 4] and [-2, -4], respectively.

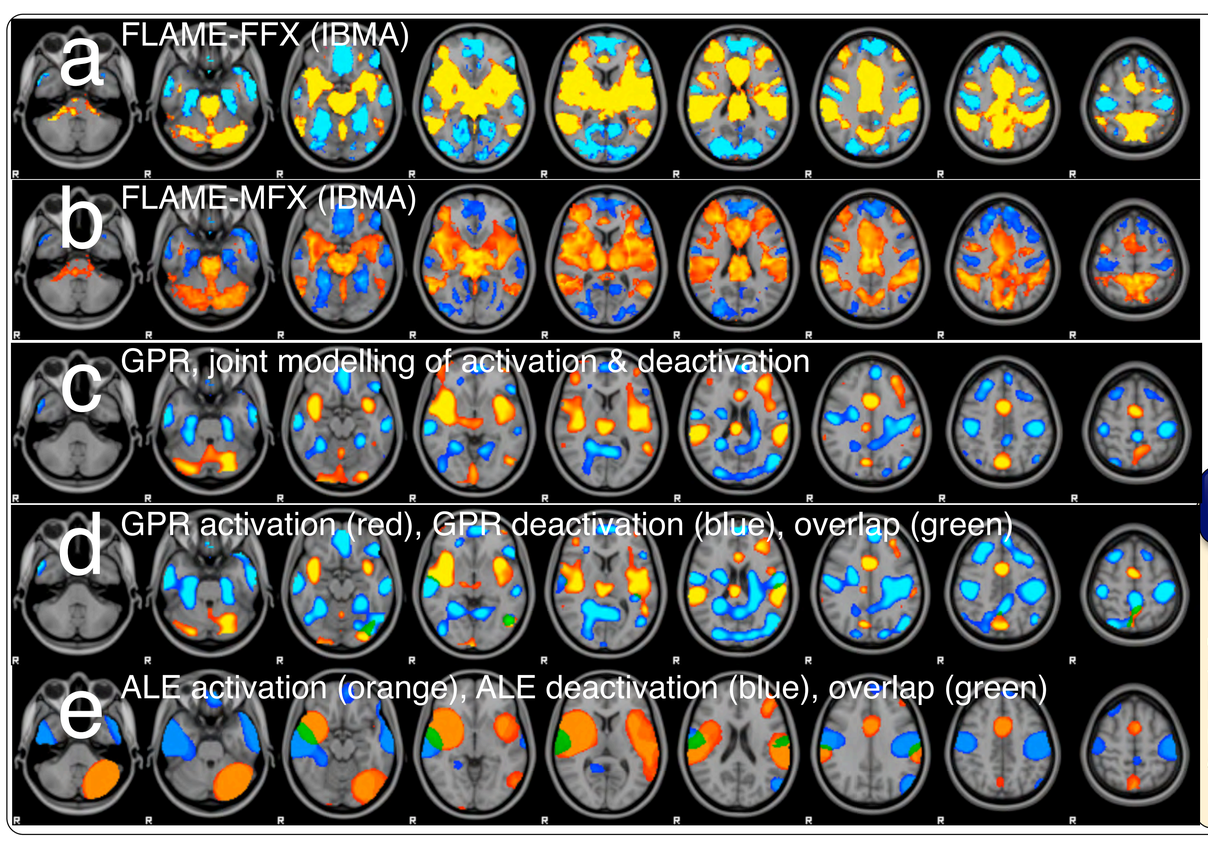

Figure 4: IBMA and CBMA results (i.e., Z-stat images) when pooling a set of 20 fMRI studies. Red-yellow and blue colours show Z-stat values with range [2, 4] and [-2, -4], respectively, and the displayed slices are selected from z=-40mm to z=40mm, every 12mm in MNI coordinates. While none of the CBMA methods can perfectly reproduce the IBMA results, the GPR appears much more similar than ALE; further, when activation and deactivation are modelled separately, ALE has several areas where it finds both activation and deactivation.

References

[1] G. Salimi-Khorshidi, et al. "Using Gaussian-Process Regression for Meta-analytic Neuroimaging Inference Based on Sparse Observations", *IEEE Trans. on Med. Imaging*, 2011.
[2] G Salimi-Khorshidi, et al. "Meta-analysis of neuroimaging data: A comparison of image-based and coordinate-based pooling of studies." *NeuroImage*, 45(3):810--823, 2009.